

# Nitrate Removal from Water using Exchange Resins

CRISTINA MODROGAN\*, OANAMARI DANIELA ORBULET, ALEXANDRA RALUCA MIRON

University Politehnica of Bucharest, Faculty of Applied Chemistry and Materials Science, Department of Analytical Chemistry and Environmental Engineering, 1-7 Polizu Str., 011061, Bucharest, Romania

*Nitrates are very soluble and do not bind to soils, therefore, they have a high potential to migrate to groundwater sources. When these groundwaters are purposed for potable drinking water sources, the presence of nitrates can pose serious health risks, especially for infants and pregnant women. The main purpose of this paper is the study of nitrate removal from contaminated waters using two ion exchangers (A520 E and A 100). The equilibrium process can be well described by both Freundlich and Langmuir models, at 20 and 30°C. The dependence of thermodynamic water retention capacity on the concentration of a solute is to be described by an e-function experimentally confirmed in the literature. Process parameters including temperature and the initial concentration were examined and the obtained data being modeled using three kinetic models, respectively the pseudo-first-order equation, the pseudo-second-order and the pore diffusion. The best experimental adsorption data were obtained by means of pore diffusion and pseudo-second-order models.*

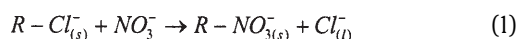
*Keywords: Purolite A 520 E and A 100, nitrate, ion exchange, pollution prevention, kinetic study*

Wastewater from fertilizer production contains a considerable amount of nitrogen in the ammonia and  $\text{NO}_3^-$  form. It also contains a certain amount of fluorides,  $\text{NO}_3^-$ , phosphates, silica and suspended matters [1]. Recent results obtained by some investigators refer to the mechanism of  $\text{NO}_2^-$  enzymatic reduction of the nitrogen oxides. One of the common processes in wastewater treatment, recently used, is the ion exchange [2, 3]. The ion exchange process has been satisfactorily used for municipal water treatment. [4]. As proven by data contained in the specialized literature the ion exchange is a very effective process which can be used in removing  $\text{NO}_3^-$  from water. This removal procedure can be used in a lot of concentrations.

The increased  $\text{NO}_3^-$  concentration in public water supplies presents a potential health hazard due to the nitrites reduction in the gastrointestinal tract. In its turn,  $\text{NO}_3^-$  is a potential health hazard to infants [5, 6] and pregnant women due to  $\text{NO}_3^-$  reduction to  $\text{NO}_2^-$ , in the infants stomach, which can bind with the hemoglobin of the affected babies, thus diminishing the oxygen transfer to the body's cells resulting in a bluish skin color often called methemoglobinemia or "the blue baby syndrome" [7, 8].

Under certain circumstances, the  $\text{NO}_3^-$  can be converted into the much more poisonous  $\text{NO}_2^-$  and ultimately even to a carcinogenic nitrosamine ([9-12] which primarily affects the esophagus and pharynx (gastrointestinal tract).  $\text{NO}_2^-$  and  $\text{NO}_3^-$  are also frequently used as meat preservatives. Cooking meat (which contains  $\text{NO}_3^-$  and  $\text{NO}_2^-$  as preservatives) favors the nitrosamine formation. Figure 1 presents the  $\text{NO}_3^-$  migration in human body.

For the  $\text{NO}_3^-$  removal from water, the basic anionite chloride form (A520 E) and the weak basic anionite chloride form (A 100) are known [14 - 18]. The first one is  $\text{NO}_3^-$  ion selective while the second one is nonselective. In both cases, the ion exchange reaction is:



where:

R - solid matrix of the two anionites;  
(s) and (l) - solid phase and liquid phase (aqueous solution respectively).

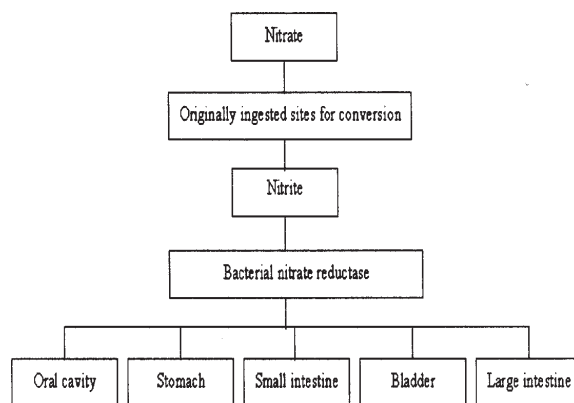


Fig. 1.  $\text{NO}_3^-$  migration in human body [13]

In order to determine the retention capacity in equilibrium for the two anions, the mass balance equation is used:

$$q = \frac{V \cdot (C_i - C_e)}{m} \quad (2)$$

where:

q - the anionite retention capacity (mg/g);  
V - the volume of the solution (L);  
 $C_i$  and  $C_e$  - the  $\text{NO}_3^-$  ion initial and respectively final concentration (mg/L);  
m - the anionite mass (g).

The conditions to contact the anionites with the solution containing  $\text{NO}_3^-$  ions were practically the same, to allow accurate comparison of performance.

The aim of the undertaken theoretical and experimental studies was to investigate the performances of two ion exchanger, A 520 E and A 100, having nitrate removal as a goal.

## Experimental part

The strong base  $\text{NO}_3^-$  selective anion exchanger Purolite A 520E and the weakly basic anion exchanger, Purolite A 100, were kindly provided by Purolite Int. Ltd. The A 520 E is a macroporous strong basic anion resin, which is specially designed for nitrates removal from water and shows more affinity for  $\text{NO}_3^-$  ions than the other anions. The A 100 exchanger is a macroporous weakly basic anion exchange.

\* email: c\_modrogan@yahoo.com

Physico-chemical properties	Purolite A-520E	Purolite A-100
Polymer Matrix Structure	Macroporous, styrene-divinylbenzene	Macroporous, styrene-divinylbenzene
Functional groups	Quaternary ammonium	Tertiary amine
Ionic form, as shipped	Cl <sup>-</sup>	Free base
Physical form and appearance	Opaque cream spherical beads	Opaque hard spherical beads
Temperature limit	max. 100°C	max. 100°C
pH Range, stability	0 – 14	0 – 14
pH Range, operating	4.5 – 8.5	0 – 9

**Table 1**  
PHYSICO-CHEMICAL PROPERTIES OF  
PUROLITE ION EXCHANGER

The physico-chemical properties of the two ion exchangers offered by the Purolite (10) are presented in table 1.

The experiments regarding the equilibrium of the ion exchange processes and their related kinetics were performed on a non-stationary system (batch conditions), in a continuously stirred (300 rpm) glass thermostated vessel (capacity of 100 mL, the thermostated accuracy was  $\pm 1^\circ\text{C}$ ). The  $\text{NO}_3^-$  concentration was periodically determined by UV-VIS spectrophotometer (Cintra 5). All used reagents were analytically pure. They were purchased from Sigma-Aldrich. Distilled water was used for the solutions.

All experiments were carried out in duplicate sets and all analyses were performed in parallel within each set.

The ion exchange tanks are filled with resin beads. The resin bead consists of a styrene – divinylbenzene copolymer attached to a quaternary amine functional group. Before the resin is exposed to contaminated water, the functional group is bonded to chloride ion.

#### Adsorption isotherms determination

In order to study the ion exchange equilibrium, the ion exchange isotherms were determined. For this purpose the  $\text{KNO}_3$  solutions (10 samples) of different concentrations (between 5 and 100 mg/L) were prepared.

Each experiment consists of the contact between the 50 mL  $\text{KNO}_3$  solution of known concentration and 0.05 g resin.

The resin-solution system was stirred in the thermostated vessel during 24 h, enough to reach the equilibrium. Each sample was spectrophotometrically analyzed, and the resin loading was calculated using equation (2).

#### Kinetic study

0.05g ion exchanger were in contact with 50 mL  $\text{KNO}_3$  (concentration 50 and 100 mg/L) in Erlenmeyer jar. The samples were stirred at 300 rpm for 5, 10, 20, 30, 60 and 90 min using a Heidolph Unimax shaker. The experiments were carried out at 20 and 30°C. After mixing, samples were filtrated using blue ribbon filter paper and brought to a 50 mL flask. 10 mL samples from the filtrate were taken and spectrophotometrically analysed. The method of analyse is based on the colour reaction between disulphonic phenol acid and nitrate ions in solution which leads to the formation of a yellow nitro aromatic derivative.

The coloured samples were spectrophotometrically analyzed. The calibration curve was achieved first. Samples of 0.25, 0.5, 1, 5, 10, 25 mL were taken from the standard working solution and brought to volume with distilled water in 100 mL calibrated flasks. From each flask, 10 mL were taken and put in vessels to evaporate on water bath until they dried. 0.5 mL disulphonic -phenol acid was added to the residue left after evaporation and kept motionless 15 min for cooling. Then 1 mL ammonia was added, until the full colour development. The solution was brought to volume with distilled water in 25 mL calibrated flasks and photo-metered at  $\lambda = 410 \text{ nm}$ .

For analysis, the samples were treated the same way, and after the colour development, they were sufficiently diluted to fit the scale. The samples were then photo-metered at  $\lambda = 410 \text{ nm}$ , thus determining the  $\text{NO}_3^-$  concentration.

## Results and discussions

### Equilibrium studies

The equilibrium adsorption isotherm is important in the adsorption system design. The distribution of  $\text{NO}_3^-$  between the liquid and the solid phase in equilibrium is expressed by the Freundlich and Langmuir models. These equations are widely used, the former being empirical while the second assumes that the maximum adsorption occurs when the surface is covered by the functional groups.

Langmuir developed a theoretical equation, considering that a monomolecular adsorption layer occurs on an energetically homogeneous surface, and that there is no interaction between the adsorbed molecules. The Langmuir adsorption isotherm plot ( $q_e$  vs.  $C_e$ ).  $C_e$  (figs. 2 and 3) indicates the applicability of Langmuir adsorption isotherm. The values of  $q_m$  and  $b$  were calculated from the slope and the intercept of the linear plots  $C_e/q_e$  vs.  $C_e$  (table 2). To predict the adsorption efficiency of the adsorption process, the dimensionless equilibrium parameter was determined by using the following equation:

$$q_e = \frac{q_m \cdot b \cdot C_e}{1 + b \cdot C_e} \quad (3)$$

where:

- $q_e$  - the adsorbent equilibrium concentration (mg/g);
- $q_m$  - the adsorbent capacity for a monolayer adsorption (mg/g);
- $b$  - equilibrium constant;

Ion exchanger	Langmuir, 20°C			Langmuir, 30°C		
	q <sub>m</sub>	b	R <sup>2</sup>	q <sub>m</sub>	b	R <sup>2</sup>
A 520 E	38.5	0.046	0.90	51.92	0.012	0.98
A 100	40.5	0.049	0.84	45.21	0.016	0.87

Ion exchanger	Freundlich, 20°C			Freundlich, 30°C		
	R <sup>2</sup>	k	n	R <sup>2</sup>	k	n
A 520 E	0.91	0.046	0.98	0.87	11.8	1.27
A 100	0.80	0.049	0.97	0.76	19.7	1.19

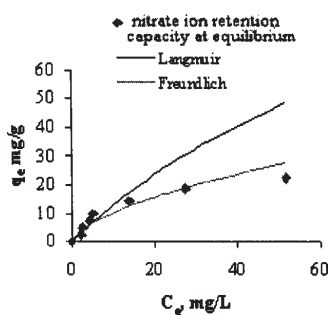


Fig. 2. Equilibrium isotherms for NO<sub>3</sub><sup>-</sup> - Purolite A520E at 20°C

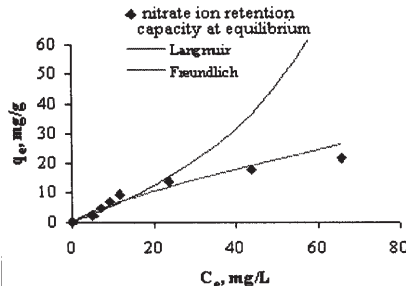


Fig. 3. Equilibrium isotherm for loading NO<sub>3</sub><sup>-</sup> onto Purolite A 100 at 20°C

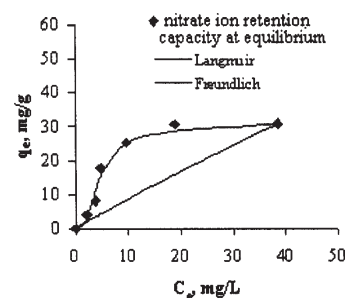


Fig. 4. Equilibrium isotherm for loading NO<sub>3</sub><sup>-</sup> onto Purolite A520E at 30°C

Table 2  
LANGMUIR EQUILIBRIUM  
PARAMETERS AT 20 AND 30°C

Table 3  
FREUNDLICH EQUILIBRIUM  
PARAMETERS AT 20 AND 30°C

$C_e$  – the equilibrium concentration in liquid phase (mg/L).

The Langmuir adsorption isotherm model may be rearranged as follows:

$$\frac{C_e}{q_e} = \frac{1}{q_m \cdot b} + \frac{C_e}{q_m} \quad (4)$$

Table 2 shows the thermodynamic parameters calculated using the Langmuir isotherm at 20 and 30°C respectively.

The Freundlich model is an indicative of the sorbent surface behaviour. The Freundlich equation, which is an empirical one, is as follows:

$$q_e = K_f \cdot C_e^{(1/n)} \quad (5)$$

where  $K$  and  $n$  are constants which were experimentally determined.

$$\log q_e = \log K_f + \frac{1}{n} \cdot \log C_e \quad (6)$$

where  $K_f$  and  $1/n$  are Freundlich constants in respect to the adsorption capacity and adsorption intensity, respectively.

The resin behaviour showed a better fit to the Langmuir isotherm than the Freundlich one.

Table 3 shows the empirical Freundlich equation coefficients (4) as obtained by logarithmic transformation.

The isotherms obtained by fitting the experimental data using the two isotherms reveal that Langmuir isotherm are more in line with the experimental results.

Comparing isotherms 2-5 the high exchange capacity of the strongly basic resin A520 for NO<sub>3</sub><sup>-</sup> anion versus the weak basic resin A 100 could be observed. The adverse effect of temperature increase on the exchange capacity was also noticeable.

The experimental data are presented in figure 2-5 in  $q_e - C_e$  coordinates, where  $q_e$  is the ion exchange loading at equilibrium, mg/g, and  $C_e - \text{KNO}_3$  concentration at equilibrium, mg/L.

As expected, the adsorption capacity,  $q_m$ , in monomolecular layer, is higher for A 520 E anionite. This fact was verified using the linearized Langmuir equation. The resin showed a better fit for the Langmuir isotherm than the Freundlich isotherm. The results are virtually identical to those obtained by fitting the experimental results presented in figure 3.

The anionite A520 E has also the advantage of a higher selectivity of the NO<sub>3</sub><sup>-</sup> compared to other anions such as SO<sub>4</sub><sup>2-</sup> [14] and that is why the resin is recommended as an ideal option for the treatment of water containing nitrates.

The aspect of the ion exchange isotherms shown in figure 2 indicates that both anion exchangers in Cl<sup>-</sup> form have a good capacity of NO<sub>3</sub><sup>-</sup> retention by ion exchange, but the values are strongly influenced by the exchanger type. The anion exchanger A520 retains a larger amount of NO<sub>3</sub><sup>-</sup> than the anion exchanger A 100. The removal efficiency increases to an optimum dosage beyond which the removal efficiency is negligible. The NO<sub>3</sub><sup>-</sup> concentration at equilibrium in solution increases with the increasing initial concentration of in initial solution.

The ion exchange isotherms shown in figure 3 have the same form up to 30 mg/L concentration and show similar values for the capacity of NO<sub>3</sub><sup>-</sup> retention from water under static conditions, although total capacities and morphologies are different. On the other hand the amount of NO<sub>3</sub><sup>-</sup> removed from water is almost identical in the case of both ion exchangers.

#### The kinetic study of ion exchange process

In order to characterize the process from the kinetical point of view, curves were obtained using the experimental apparatus described above.

The process efficiency is controlled by the kinetics of adsorption and hence the several kinetic models are available to predict the mechanism involved in the sorption process. Among these models, there are pseudo first order, pseudo second order and interparticle diffusion, rate equation [19].

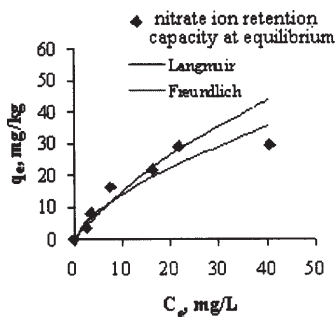


Fig. 5. Equilibrium isotherm for loading  $\text{NO}_3^-$  onto Purolite A 100 at  $30^\circ\text{C}$

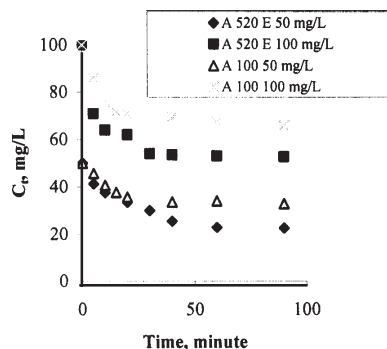


Fig. 6. The temperature influence on the  $\text{NO}_3^-$  sorption kinetics at  $20^\circ\text{C}$

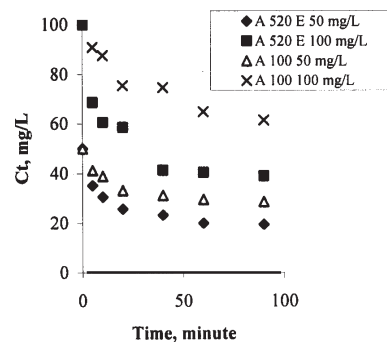


Fig. 7. The temperature influence on the  $\text{NO}_3^-$  sorption kinetics at  $30^\circ\text{C}$

Kinetic model parameters		Temperature	
		$20^\circ\text{C}$	$30^\circ\text{C}$
A 520 E			
Pseudo first order	$k_1$	0.235	0.0340
	$r^2$	0.986	0.979
Pseudo second order	$k_2$	0.033	0.016
	$r^2$	0.999	0.984
Pore diffusion	$k_p$	5.949	6.141
	$r^2$	0.991	0.986
A 100			
Pseudo first order	$k_1$	0.013	0.042
	$r^2$	0.973	0.837
Pseudo second order	$k_2$	0.031	0.064
	$r^2$	0.968	0.979
Pore diffusion	$k_p$	6.138	5.103
	$r^2$	0.989	0.992

**Table 4**  
KINETIC MODEL PARAMETERS FOR THE ADSORPTION OF NITRATES AT DIFFERENT TEMPERATURES ON A 520 E AND A 100

Pseudo-first-order:

$$\log(q_e - q_t) = \log q_e - \frac{k_1}{2.303} t \quad (7)$$

Pseudo-second-order:

$$\frac{t}{q_t} = \frac{t}{q_e} + \frac{1}{k_2 q_e^2} \quad (8)$$

The interparticle diffusion model was applied to different adsorption systems and was adequate to the adsorption systems [20]:

$$q_t = k_p t^{0.5} \quad (9)$$

Samples were taken after 5, 10, 20, 30, 60 and 90 minutes, the results of the experiments being presented in figure 6 and 7.

Curves in figure 6 and 7 reveal that the ion exchange rate is higher in the case of strongly basic resin A 520 E, having a higher exchange capacity. The higher temperature has a positive influence on the ion exchange rate.

The experimental data on ion exchange kinetics for anion exchanger samples with macro-porous morphology Purolite A520 E, strong basic, and A100, low basic, are shown in figure 6, as a function of  $\text{NO}_3^-$  concentration in solution versus time. The kinetic curves have a similar shape and reveal a high ion exchange rate at the beginning of the process. The decrease of the ion exchange rate is correlated to the decrease of concentration in solution

and with the progress of  $\text{NO}_3^-$  the system towards the equilibrium state.

Figure 7 shows the different variations of  $\text{NO}_3^-$  concentration in time. The relative similar behaviour between the two samples in terms of kinetics in the first 20 min of the ion exchange process is likely due to the similar morphology (macroporous type) and the fact that the ion exchange process is controlled by internal diffusion.

Several kinetic models including pseudo first order, pseudo second order and pore diffusion were used for the simulation of the experimental data. The kinetic parameters calculated from equations 7-9 for the adsorption of  $\text{NO}_3^-$  at different temperatures and in different concentrations on Purolite A 520 E and A 100 are given in table 4. The pseudo second order and pore diffusion models successfully fit the adsorption kinetic.

#### Temperature effect

The temperature influence on the adsorption process is associated with several thermodynamical parameters. Table 4 shows an increasing trend of  $\text{NO}_3^-$  removal by the temperature increase from 20 to  $30^\circ\text{C}$ . The increase in  $\text{NO}_3^-$  uptake may be due to the increasing rates of intraparticle diffusion of sorbate ions into the adsorbent pores at higher temperature; it may also be attributed to the enlargement of the pore size and/or the activation of the adsorbent surface [21]. The rates of several chemical reactions

seriously increase with the few degrees temperature increase [12].

## Conclusions

This paper is a study of the possibility to remove the  $\text{NO}_3^-$  ion from fresh water by ion exchange using a strongly basic anionite, Purolite A 520 E and a weak basic one, Purolite A 100.

Initially, the adsorption rate of nitrates onto A 520 E and A 100 was very high, followed by decreasing rates, until an almost constant value was reached.

The analyses on the ion exchange capacity in equilibrium shows a better retention of the ion exchanger A 520 in comparison with A 100 one.

The performances of A 520 in respect to ions in relation to  $\text{NO}_4^{2-}$  [14] recommend its use in a selective water treatment containing both anions. When selectivity is not significant resin A 100 can also be used.

The adsorption kinetic confirms the better retention of Purolite A 520 E, both in terms of ion exchange rate and exchange capacity.

The increasing temperature determines the increasing of the ion exchange rate for both A 520 E and A 100 resin.

The adsorption process obeys the Langmuir isotherm. As a result, the groundwater containing a lower  $\text{NO}_3^-$  concentration than the permissible level for drinking water is purified using Purolite A 520E. The ion exchange process based on Purolite A 520E and A 100 can be applied more widely and economically in small-scale water suppliers for  $\text{NO}_3^-$  removal.

The comparative kinetic data reveal that the ion exchange kinetics is still differentiated for the two samples: in the same conditions, the ion exchange rate is higher for strong basic anion exchanger (Purolite A520 E) although both have a macro-porous morphology. Temperature influences positively the  $\text{NO}_3^-$  sorption kinetics.

As a result, the groundwater containing a lower  $\text{NO}_3^-$  concentration than the permissible level for drinking water is treated with Purolite A 520E and A 100.

The adsorption isotherms of nitrates were better fitted by the Langmuir model under the considered conditions.

Among the three models, the pseudo-second-order appears to be the most convenient for describing the adsorption kinetics of nitrates on A 520 E.

*Acknowledgements: The work has been funded by the Sectoral Operational Programme Human Resources Development 2007-2013*

*of the Ministry of European Funds through the Financial Agreement POSDRU/159/1.5/S/134398.*

## References

- 1.KROISS, H., NEGM, M, Water Research, **28**, 1994, p. 2209-2217.
- 2.PHILPOT J. M., DE LARMINANT G., Water Supply, **6**, 1998, p. 45-50.
- 3.CLIFFORD D., XIAOSHA L., Journal of American Water Works Association, **85**, 1993, p. 135-143.
- 4.ANDREWS D.A., HARWARD C., Journal Instr. Water Environment Management., **8**, 1994, p. 120-127.
- 5.HALLING-SORENSEN, B., NIELSEN, S.N., LANZKY, P.F., INGERSLEV, F.L., LUTZHOFF, H.C., JORGENSEN, S.E., Chemosphere, **36**, 1998, p. 357-393.
- 6.CHAN, T.Y.K., Southeast Asian Journal of Tropical Public Health, **27**, 1996, p. 189-192.
- 7.BENEFIELD L. D., JUDKINS J.F., WEAND, B. L., Printice-Hall, Inc., Englewood Cliff, N.J. (1982)
- 8.MODROGAN C., DIACONU E., ORBULEȚ O. D., MIRON A. R., Rev. Chim. (Bucharest), **61**, no. 6, 2010, p. 580
- 9.LEAKOVIC S., MIJATOVIC I., CERJAN-STEFANOVIC Š., HOD•IC E., Water Research, **34**, 2000, p. 185-190.
- 10.MATSUMOTO, G. I., NAKAYA S., MURAYAMA, H, MASUDA, N., KAWANO T., WATANUKI, K., TORII T, Proceedings of the National Institute of polar Research Symposium in Polar Biology, **5**, 1992, p. 125-145.
- 11.NEWBORNE P.M., Trace Substances and Health A hand book Pt-2. Marcel Dekker, New York, 1982, pp. 1-46.
- 12.RICHARD Y., Journal Institution of Water and Environmental Management **3**, 1989, p. 154-167.
- 13.NIESINK, R.J.M., VRIES, J., HOLINGER, M.A., Toxicology: principles and applications, New York: CRC Press; Boca Raton, 1996, pp. 1284.
- 14.CEICĂ A., BULGARIU L., LAZĂR L., CREȚESCU I., BALASANIAN I., Buletinul Institutului Politehnic din Iași, Tomul LXI (LX), **4**, 2010, pp. 119-131.
- 15.SABA S., NALAN K., UMRAN Y., ARDA M., MITHAT Y., Reactive & Functional Polymers, **66**, 2006, p. 1206-1214.
- 16.SILAGHI-DUMITRESCU R., Revue Roum. Chim., **54**, 2009, p. 513
- 17.STEFAN, D. S., PINCOVSCHI I., Rev. Chim. (Bucharest), **64**, no.12, 2013, p. 1381
- 18.DRAGAN, G., Rev. Chim. (Bucharest), **61**, no. 9, 2010, p. 897
- 19.AHMARUZZAMAN M., D.K. SHARMA, J. Coll. Interf. Sci., **287**, 2005, p. 14-24
- 20.YANG X., AL-DURI B., J. Coll. Interf. Sci., **287**, 2005, p. 117-127
- 21.NAMASIVAYAM C., YAMUNA R. T., Chemosphere, **50**, 2003, 517-528.
- 22.ARSLANOGLU F.N., KAR F., ARSLAN N., J. Food Eng., **71**, 2005, p. 156-163

Manuscript received: 17.02.2014